Macromolecules

Article

pubs.acs.org/Macromolecules

Minimal Model of Intrinsic Chirality to Study the Folding Behavior of Helical Polymers

Christian R. Boehm and Eugene M. Terentjev*

Cavendish Laboratory, University of Cambridge, JJ Thomson Avenue, Cambridge CB3 0HE, U.K.

ABSTRACT: We describe a minimal model of an intrinsically chiral polymer chain, and characterize its equilibrium and transient behavior at different temperatures, and in effective solvent environments by means of Brownian dynamics simulation. By contrast to previous studies, our model transparently includes intrinsic curvature and torsion as a measure of residue-inherent (molecular) chirality to establish a defined handedness, while allowing the observation of a transformation between a high-temperature expanded random coil and a dense helical or globular state at low temperatures. In fair or good solvents, a straightforward denaturation of a folded helix toward a random coil is observed. In poor solvent, this process is superimposed by adoption of a condensed globule in the low-medium temperature range. Under these conditions, we find that helical chains represent metastable states separated from the thermodynamically favored dense globule by an energy barrier. Finally, by combining the observations of structural transformations with the evidence of thermodynamic anomaly in the heat capacity, we suggest that the helix−globule transformation represents a discontinuous phase transition-like process.

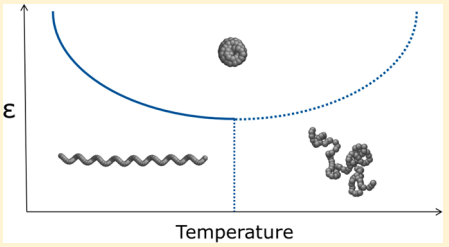

INTRODUCTION

Proteins arguably constitute the most extensively studied class of biomacromolecules due to their involvement in nearly every biological process and their manifold potential applications in biotechnology and medicine. As a consequence, the prediction of native structures from a primary sequence, the so-called *protein folding problem*, has been under extensive investigation for more than 5 decades.[1] Protein folding may be defined as the coordination of the many degrees of freedom of a flexible polymer chain into a well-defined and compact conformation based on energetics specified by its linear amino acid sequence.[2] Thereby, formation of secondary structure elements constitutes the first step from a one-dimensional random chain toward a characteristic three-dimensional folded structure. In particular, right-handed helical secondary structure appears as the prevalent motif in the native conformational space of polypeptides and long proteins. The most abundant helical configuration, the α-helix, accounts for approximately 31% of amino acid secondary structures alone, with another 4% of helices natively being in 3_{10}-helical conformation.[3] However, the helix as a structural motif is not exclusive to proteins: it is similarly prevalent in DNA and RNA[4−6] and in many polysaccharides. Arguably, helical structures derive their apparent universal biological significance from allowing natively linear polymers to maximize their thermodynamic stability in a poor solvent environment (i.e., low temperature, unfavorable pH, or salinity) by means of extensive intra- or intermolecular bonding. The helical shape of nucleic acids has been thought to principally arise from a complex interplay of interbase hydrogen bonding and coaxial hydrophobic nucleobase stacking,[7] while helicity in polypeptides appears to be stabilized mostly by intramolecular hydrogen bonding between each carbonyl oxygen and its complementary amino nitrogen at the fourth residue toward the C-terminus, in addition to steric repulsion between subsequent side-chain residues.[8] However, it is surprisingly seldom that a connection is made between an inherent molecular chirality of monomeric units (residues) involved in these biopolymers and their native fold characterized by a "phase chirality" of the secondary structure.[9]

Since the discovery of the α-helix in 1950,[10] the thermodynamic stability and kinetic behavior of helical secondary structure in biopolymers has been extensively addressed in theoretical models and numerical simulations.[11,12] Generally speaking, helix−coil transition models seek to describe conformations of linear polymers in solution based on a statistical mechanics approach. They allow estimation of the relative fraction of a model chain which assumes a helical state−characterized either by a distinct rotating pattern in geometric parameters and/or specific hydrogen bonding−instead of a randomly ordered coil state under various experimental conditions and intrinsic constraints.[13] The majority of theoretical approaches to the helix−coil transition developed over the past 50 years is derived from the 1D-Ising model.[14] In large part, such models consider particles as helix residues or segments, and their respective two-state variables to represent the distinct states of helix/coil, or hydrogen-bonded/non-hydrogen-bonded. The first prominent category of helix−coil models, referred to also as ZB models, follows from Zimm−Bragg in 1959.[15] It considers the cooperativity among subsequent monomer states as basis for calculation of average fractional helicity. In other words, the model distinguishes between helix nucleation and helix propagation, and appreciates

Received: April 7, 2014
Revised: July 5, 2014
Published: August 21, 2014

   dx.doi.org/10.1021/ma500720t | *Macromolecules* 2014, 47, 6086−6094

that the probability for a segment assuming the helical state is dependent on the state of neighboring units. By contrast to the ZB category of helix−coil models essentially counting hydrogen bonds, LR-type models pioneered by Lifson and Roig count specific residue conformation changes between a helix and a coil state.[16] The original LR model constitutes a refinement to Zimm−Bragg in that an α-helix is only stabilized by a hydrogen bond if three consecutive units have adopted helical conformation. One notable modification subsequently made includes additional independent terminal capping parameters n and c, which equal 1 in the original LR formulation.[17] Both main categories of helix−coil models suffer from a similar limitation: Being derived from the 1D-Ising model in their essence, they are incapable of describing true thermodynamic phase transitions since indefinite helix growth and long-range order are not possible in 1D according to the Mermin-Wagner theorem.[18] Furthermore, the coarse-grained nature of the ZB and LR approaches does not constitute an entirely convincing approach to capturing the fundamental physics orchestrating the balance between the energy gain of residue interactions, the energy cost of stiff chain bending, and the entropy of a polymer random walk. Recent work on numerical simulation of the helix−coil transition within the ZB framework, though based on realistic potentials, may in particular be limited by intrinsically nonchiral Hamiltonians producing polymer conformations of random handedness.[19] To favor a helical ground-state at low temperatures, directional interactions with chiral symmetry must be engineered into the system. The fact that neither common ZB and LR category models of the helix−coil transition, nor of DNA denaturation, consider the inherent chirality of constitutive residues linked to the emergence of helical conformations is their significant limitation.[20]

Chirality is an inherent characteristic of nature. A lack of inversion symmetry in systems not exhibiting any dipolar or vector property can be observed across many length scales, from asymmetric carbon atoms to spiral galaxies. On the molecular scale, this breaking of symmetry has been a source of interest in various fields, from mathematics to chemistry and medicine, since the phenomenon was first discovered by Pasteur in 1848.[21] The arguably most palpable impact of chirality is the fact that enantiomers often have different and even opposite functional properties in biology. A pair of enantiomers differs in electronic properties and shape only in a very subtle way, leaving handedness-sensitive molecular interactions very weak. However, it is this slight difference in intermolecular forces between chiral chemical compounds within biological systems which provokes their distinct physiological effects. It appears obvious that the invariable presence of specific chirality in fundamental modular building blocks of life, amino acids and nucleotides, would shape the structure of their respective biopolymers and hence the function of all living systems. Homochirality may be seen as a requirement or a result of replication in living systems, and the mechanism underlying its emergence is still discussed.[22]

It is well accepted that macroscopic helicity (phase chirality) is linked to the handedness of respective building blocks, such as D-sugars in DNA or L-amino acids in proteins, and this link is supported by several experimental studies.[9,23,24] However, careful qualification of the relative contributions of hydrogen bonding, base stacking, steric effects, or monomeric handedness to macromolecular secondary structure could greatly enhance the physical understanding of the relationship between homochirality and helicity, and potentially improve the insight into the emergence of asymmetry in living systems. The investigation of minimal biopolymer models represents a meaningful approach to this question, as individual structural and dynamical properties which may represent the essence of helicity can be studied independently. Though sequence heterogeneity certainly plays an important role in defining the native conformation of biopolymers, the physical forces and effects at the base of polymer morphology are universal. Thus, minimal models may be used to establish a base for quantitative comparison with experimentally determined structures, which constitutes a major motivation of theoretical polymer physics. While the majority of contemporary numerical attempts to study the phase behavior of helical polymers has been based on realistic potentials,[25−29] several groups have specifically explored minimal models in the past 2 decades. Kemp et al.[30] proposed their freely rotating chain-type minimal model ignoring the specifics of amino acids in 1998. It features a chain Hamiltonian shaped by a short-ranged chiral interaction, implemented as triple product of three consecutive tangent segments raised to an arbitrary power, and allows observation of four different phases using multicanonical Monte Carlo simulation. This model demonstrates that helix foldability may increase with anisotropy in the potential function, and undergoes discontinuous first-order-like helix−coil transitions.[31,32] Varshney et al. have taken a similar approach, and utilized a dihedral angle cutoff to assign individual beads a negative enthalpy, thereby emulating formation of a hydrogen bond.[33] They find a rich state diagram where continuous helix−coil and coil−globule transitions become coupled at low temperature and sufficient particle interaction strength ε.[34] While both models consider torsional angles between individual residues a basis for helicity, they do not implement true intrinsic curvature κ and torsion τ, as represented in the Yamakawa theory.[35] The latter treats linear polymers with energies quadratic in the local difference from preferred intrinsic curvature and torsion, represented by local angular rates of rotations on the chain. Unfortunately, in this formalism extraction of results is not a transparent process. A simplified auxiliary field model embracing intrinsic curvature and zero-average torsion for increased transparency and utility was recently developed.[36] However, it does not implement excluded volume effects or a preferred chiral sense. Here we propose an alternative minimal model which implements both intrinsic curvature and torsion in a straightforwardly adjustable way to shape helices of defined handedness. Thereby, our model directly connects force field parameters to frame-independent geometric properties of a helical space curve (radius and pitch). We employ Brownian dynamics simulation to characterize the minimal model with respect to its transient and equilibrium thermodynamic and morphological properties, including its phase behavior.

THE MODEL

The foundation of the minimal model of a chiral polymer reported in this work is laid by its force field. Defining the form and parameters of the mathematical functions shaping the pair potential of interaction between chain monomers (residues), it takes the general form

$$E = E_{bond} + E_{angle} + E_{dihedral} + E_{nonbonded} \quad (1)$$

To account for bonded interactions along the polymer chain, we follow the established tradition and employ a hybrid term composed of the attractive finite extensible nonlinear elastic

dx.doi.org/10.1021/ma500720t | Macromolecules 2014, 47, 6086−6094

(FENE) potential and a repulsive truncated Lennard-Jones (LJ) potential cut off at $r_{ij} = 2^{1/6}\sigma$:

$$E_{bond} = -0.5K_r R_0^{\,2} \ln\left[1 - \left(\frac{r_{ij}}{R_0}\right)^2\right] + 4\varepsilon\left[\left(\frac{\sigma}{r_{ij}}\right)^{12} - \left(\frac{\sigma}{r_{ij}}\right)^{6}\right] + \varepsilon \tag{2}$$

with bond stiffness parameter K_r, maximum bond extension R_0, distance between two consecutive particles r_{ij}, LJ potential well depth ε, and LJ potential root distance σ (Figure 1). The FENE

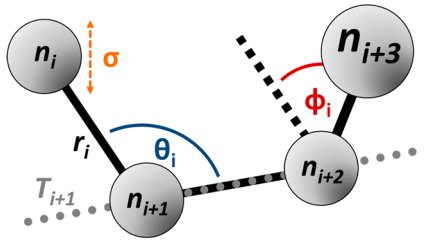

Figure 1. Schematic representation of the model chain geometry, in particular showing the direction of the tangent vector $\boldsymbol{T}_{i+1}$, the bending angle θ_i, and the torsion angle φ_i.

potential originating from the bead–spring polymer model extensively studied by Kremer and Grest is harmonic near its minimum,[37] so that the effective spring constant between monomers equals K_r. However, a FENE bond cannot be stretched beyond the maximum length R_0. This attractive potential is balanced by the repulsive portion of the LJ potential, which reflects the same excluded-volume interaction as exists between any pair of monomers (particles).

While the truncated (repulsive) LJ term is effective only between covalently linked monomers, nonbonded interactions are described by the standard LJ potential

$$E_{nonbonded} = 4\varepsilon\left[\left(\frac{\sigma}{r_{ij}}\right)^{12} - \left(\frac{\sigma}{r_{ij}}\right)^{6}\right] \tag{3}$$

to account for excluded volume effects as well as a possible effective long-range attraction between monomers in poor solvent. Again, this is standard in describing model molecular interactions. Hereby, the repulsive and attractive regions are separated by the distance σ, where the interparticle potential equals zero, and the potential minimum $-\varepsilon$ is reached at $r_{ij} = 2^{1/6}\sigma$.

While E_{bond} and $E_{nonbonded}$ accommodate polymer chains of arbitrary conformation, E_{angle} and $E_{dihedral}$ were chosen to characterize the intrinsic curvature κ and torsion τ for generation of a helical ground state. It is the combination of intrinsic curvature and torsion that shapes the macroscopic (phase) chirality in a helical polymer chain—neither of the two terms are sufficient on their own.[35] We account for bending stiffness by means of a harmonic potential for each pair of connected bonds:

$$E_{angle} = K_\theta(\theta_i - \theta_0)^2 \tag{4}$$

with bending stiffness parameter K_θ, bond angle θ_i, and equilibrium bond angle θ_0. It can be shown that E_{angle}, though simple in its mathematical form, indeed constitutes a measure of intrinsic curvature κ using geometrical considerations based on the angle between subsequent tangent vectors $\boldsymbol{T}_i$ along the chain:

$$E_{angle} = K_\theta\left[180^\circ - \cos^{-1}\left(\frac{-(\kappa\,\|\,\mathbf{T}_i\,\|)^2 + 2\,\|\,\mathbf{T}_i\,\|}{2\,\|\,\mathbf{T}_i\,\|\,\|\,\mathbf{T}_{i+1}\,\|}\right) - \theta_0\right]^2 \tag{5}$$

To account for torsional stiffness within the minimal polymer model, a CHARMM-like dihedral potential was adopted:[38]

$$E_{dihedral} = K_\varphi[1 + \cos(\varphi_i - \varphi_0)] \tag{6}$$

with dihedral stiffness parameter K_φ, torsion angle φ_i, and the equilibrium torsion phase φ_0. The potential is characterized by a single minimum at $\varphi_i = \pi + \varphi_0$, and with $\varphi_0 = 0$ it favors the standard zigzag sequence of bond orientations in the chain. In a similar way as outlined above, it can be shown that $E_{dihedral}$ represents a measure of intrinsic torsion τ (this time, the angles between three consecutive tangent vectors $\boldsymbol{T}_i$ are relevant):

$$E_{dihedral} = K_\varphi\left\{1 + \cos\left[90^\circ - \cos^{-1}\left(\frac{\tau\left|\frac{d\mathbf{T}_i}{ds}\right|^2}{\|\,\mathbf{T}_i\,\|\,\|\,\mathbf{T}_{i+1} \times \mathbf{T}_{i+2}\,\|}\right) - \varphi_0\right]\right\} \tag{7}$$

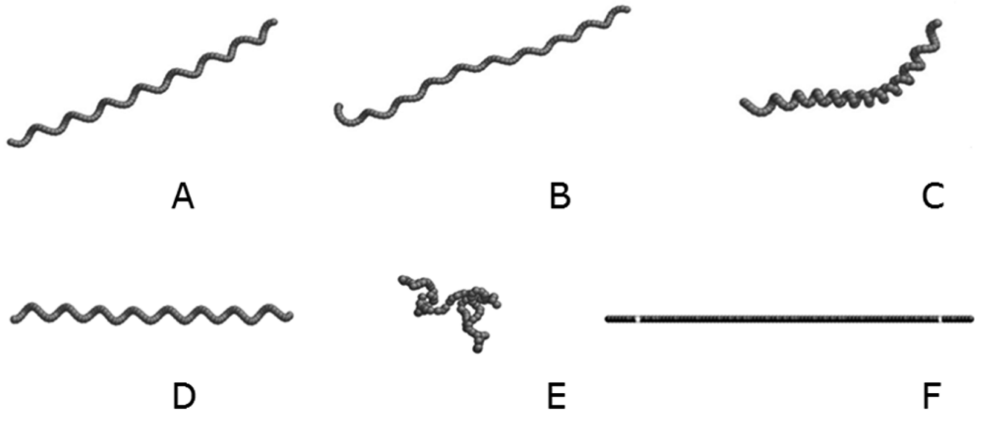

Figure 2. Structures observed after thermal equilibration of an initially straight chain at a temperature $T = 500K$ and $\varepsilon_a = 1$(kcal)/(mol) over 10^6 time steps: (A) $K_\theta = 10$ (kcal)/(mol rad^2); $K_\varphi = 10$ (kcal)/(mol), (B) $K_\theta = 10$ (kcal)/(mol rad^2); $K_\varphi = 1$ (kcal)/(mol), (C) $K_\theta = 1$ (kcal)/(mol rad^2); $K_\varphi = 10$ (kcal)/(mol). The three initial configurations used in chain simulations: (D) initial helix, (E) initial random coil, and (F) initial straight chain.

dx.doi.org/10.1021/ma500720t | Macromolecules 2014, 47, 6086–6094

Taken together, the minimal model of a chiral polymer presented here reflects both components of intrinsic (molecular) chirality, intrinsic curvature and intrinsic torsion, which may be arbitrarily shaped by target bond and dihedral angles θ_0 and φ_0, and their corresponding stiffness parameters K_θ and K_φ (see Figure 2). Unless indicated otherwise, we chose a default bending stiffness of K_θ = 10 (kcal)/(mol rad^2), and a torsional stiffness of K_φ = 10 (kcal)/(mol) for our minimal model.

Notably, intrinsic curvature and torsion as implemented in our model are related to defining geometric properties of a helical space curve of radius a and helix pitch $p = 2\pi h$, as shown below:

$$a = \frac{\kappa}{\kappa^2 + \tau^2};\ p = \frac{4\pi^2\tau}{\kappa^2 + \tau^2} \tag{8}$$

SIMULATION METHODOLOGY

In this work, we perform numerical simulations using the large scale atomic/molecular massively parallel simulator (LAMMPS) to subject a polymer chain to Brownian dynamics over time.[39,40] To perform thermal equilibration at a given target temperature, the chain is subjected to a Langevin thermostat as described by Schneider and Stoll.[41] If constrained to the microcanonical ensemble, the Langevin thermostat implements Brownian dynamics within the MD framework of LAMMPS. We simulated a polymer chain composed of N = 100 connected monomers in a large cubic cell with fixed nonperiodic boundary conditions. Unless indicated otherwise, data points represent thermodynamic averages over 10,000 ps and 6 different simulation runs each, carried out with a time step size of 1 fs. Thermal equilibration was performed at temperatures across a wide range, from 1 to 5000 K, for three different initial conformations: (i) a well-ordered helix, (ii) a straight polymer chain, and (iii) a random coil (see Figure 2) to test whether the results depend on this initial configuration. To account for deteriorating solvent conditions, the strength of the nonbonded LJ interaction between particles was increased from ε_r = 0.01 (kcal)/(mol) to ε_a = 1 (kcal)/(mol). Here we investigated an arbitrary right-handed helical ground state with θ_0 = 160° and φ_0 = 200°, corresponding to a 20° deviation from a straight chain in bending and ecliptic configuration in torsion, respectively.

EQUILIBRIUM AND THERMODYNAMICS

In essence, any investigation of polymer folding in poor solvent corresponds to an analysis of the underlying free energy landscape, which is characterized by an ensemble of conformational local minima separated by energy barriers. Natural systems generally strive for minimization of their Gibbs free energy. However, the polymer can become kinetically trapped in *metastable states* if the energy landscape cannot freely be explored (e.g., under low temperature conditions), i.e.: the system becomes nonergodic.[42] To investigate the thermodynamic properties, equilibrium potential energy PE and the average radius of gyration R_g were directly calculated as a function of temperature for different initial conformations and effective solvent environments. A remark about the "radius of gyration" is due here: the radius of gyration is a standard parameter in polymer physics reflecting the average distance of particles in the chain from their common center of mass. However, this parameter may become quite ambiguous when the equilibrium chain shape is highly anisotropic. For instance, in a liquid crystalline chain, one can identify the two principal values, $R_{g\parallel}$ and $R_{g\perp}$. In principle, the same is true in a highly elongated helix as well. However, we continue using the single-value average (in this case, $R_g = (R_{g\parallel} + 2R_{g\perp})/3$) to reduce the number of parameters to consider, understanding that this average is often dominated by the longitudinal $R_{g\parallel}$. First, we consider near-Θ solvent conditions whereby long-range attraction between monomers is negligible (ε_r = 0.01 (kcal)/(mol)).

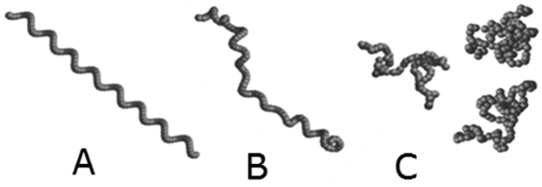

Figure 3. Prevalent chain conformations in near-Θ solvent: (A) equilibrium helix at low temperature, (B) the "melting helix", and (C) several shapes of a random coil at high temperature.

We find that the structural integrity of the initial helix (Figure 3A, $R_g \approx 16$ Å) is increasingly dissolved beyond the double-digit temperature scale, until the polymer model adopts a random coil conformation (Figure 3C, $R_g \approx 9$ Å) bare of visible helical properties over 1000 K (see Figure 4). As explained earlier, R_g represents a "radius of gyration" only for the random coil, which is spherical and random on average, while R_g is just a measure of average length for highly extended conformations such as a straight chain or a helix. At high temperatures, energy barriers of intrinsic bending and torsional stiffness can be ignored, and the initially helical polymer model adopts a fully entropy-driven conformation of an expanded random coil (self-avoiding random walk) in Θ solvent. However, since our simulations are conducted in near-Θ solvent with minor residual long-range attraction between chain monomers still present, we observe a more compact coil conformation (see Figure 4A). Considering average potential energy after equilibration (see Figure 4B), a plateau at low temperatures represents the ordered helical phase driven and dominated by the minimization of interaction energy (1), while temperatures high enough to reach the entropy-dominated regime lead to a continuous and pronounced rise of potential energy toward random coil morphology, where the Gibbs free energy is still minimized. The same qualitative equilibrium behavior is observed for all initial configurations, supporting the notion of reversibility within the process of thermally induced transformation in fair solvent.

In contrast, numerical results in poor solvent conditions characterized by an increased long-range effective attraction between monomers (ε_a = 1 (kcal)/(mol)) reveal pronounced minima of both the radius of gyration ($R_g \approx 3$ Å) and the potential energy in the low-mid temperature range, indicating an energetically favored condensed globular state (see Figure 5). It becomes apparent that this dense globular conformation becomes adopted at lower temperature for an initial random coil compared to an initial helix, which is a consequence of a minor level of thermal fluctuation being required for nucleation in the former case. This notion is supported by the results of a simulation starting from an initially straight extended chain, exhibiting thermodynamic properties very similar to the initial helix.

dx.doi.org/10.1021/ma500720t | *Macromolecules* 2014, 47, 6086−6094

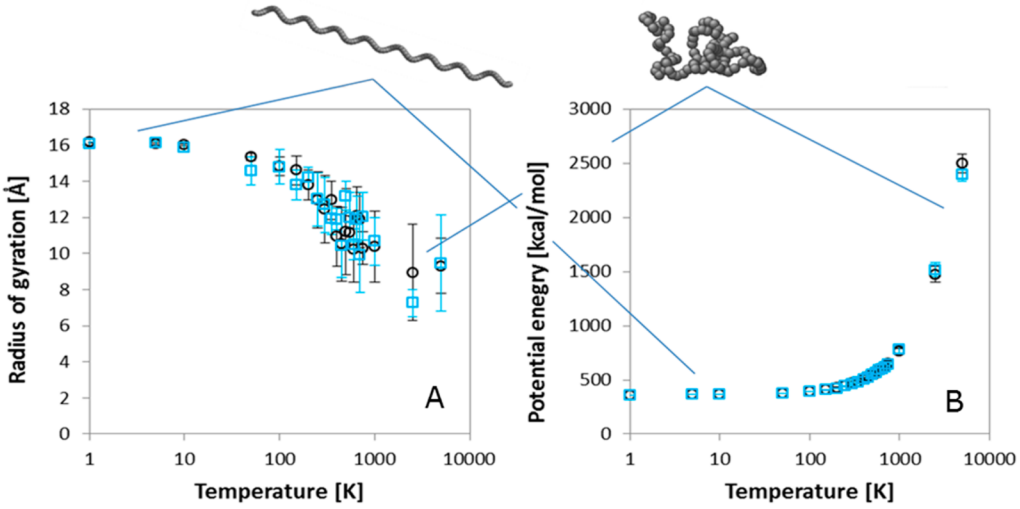

Figure 4. Equilibrium (A) radius of gyration and (B) potential energy as a function of temperature for initial helix (black circle) and initial random coil (blue square) in Θ solvent. A representative snapshot of chain conformation in different regime is showing above each plot to guide the reader.

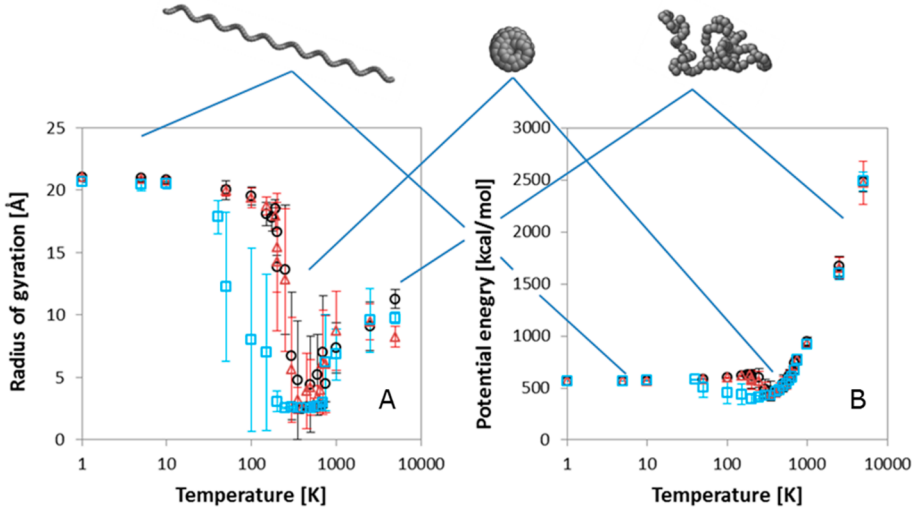

Figure 5. Equilibrium (A) radius of gyration and (B) potential energy as a function of temperature for initial helix (black circle), initial random coil (blue square), and initial straight chain (red triangle) in poor solvent.

The condensed globule is thermodynamically favored over the helical state as overall nonspecific attraction between monomers outbalances specific terms favoring bend and torsion. In this state, deviation from the "target" helical values θ_0, φ_0 is energetically unfavorable, but compensated by the combined negative energy contribution of several monomers coming together under nonbonded attraction mediated by ε_a. In contrast, in near-Θ solvent represented *via* $\varepsilon_r = 0.01\varepsilon_a$, a similar prevalence of monomer attraction over competing energy penalties does not take effect. However, as implied by the morphology of representative conformations, chain curvature remains a well-accommodated feature of the condensed globule. To obtain an indication of the mechanism of helix–globule transition, intermediate states were captured during the process of collapse (see Figure 6A).

On the basis of our observations, we hypothesize that nucleation is initiated at the polymer termini and the helix subsequently collapses into the globule alongside its axis. This process may be considered a special instance of the mechanism proposed by Halperin and Goldbart.[43] A recent detailed study of such "raindrop" coalescence has shown how a long polymer chain goes through stages of necklaces of condensed domains on its way toward the final equilibrium globule.[39] Sufficiently flexible polymer chains collapse via terminal "raindrops" in the short-chain limit,[44] as we also see in Figure 6. With increasing temperature (i.e., for temperatures greater than a "critical point" of 50 K for an initial random coil and 200 K for an initial helix

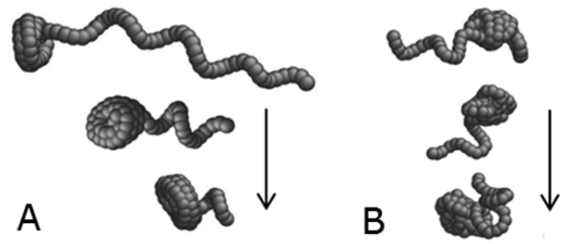

Figure 6. (A) Intermediate conformations of the helix–globule transition captured during thermal equilibration of an initial helix in poor solvent at 300 K. (B) Structures captured during thermal equilibration of an initial helix in poor solvent conditions at 700 K over 5×10^6 time steps.

dx.doi.org/10.1021/ma500720t | *Macromolecules* 2014, 47, 6086–6094

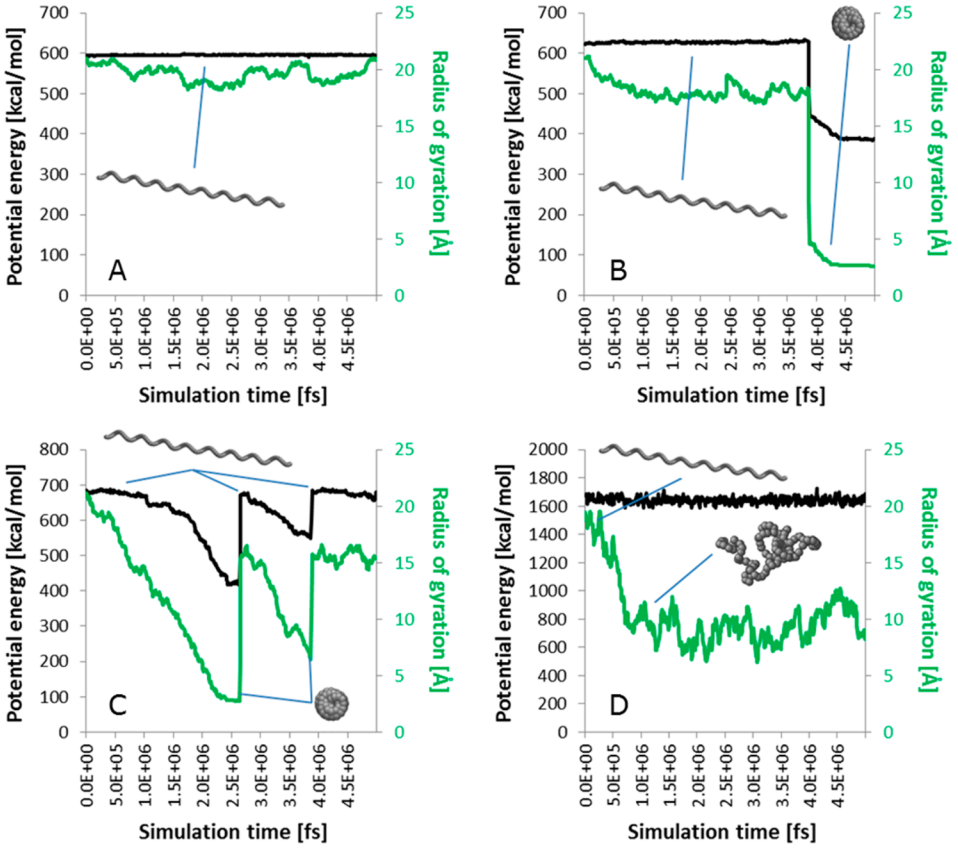

Figure 7. Characteristic examples of evolution of the radius of gyration (green) and potential energy (black) recorded from single Brownian dynamics trajectories starting from the initial helix at: (A) 100 K, (B) 200 K, (C) 350 K, and (D) 2500 K in poor solvent, ϵ_a = 1 (kcal)/(mol).

or straight chain), globular equilibrium states become continuously more amorphous and eventually resemble a random coil, again via this inhomogeneous process (see Figure 6B). The term "critical point" is used here with caution: the transformation between characteristic conformational states in a finite-size (relatively short: N = 100) chain cannot be a true critical phase transition. However, there are identifiable temperature regions where distinct conformational transformations take place, and a very sharp thermodynamic anomaly was observed at these temperatures (discussed below and illustrated in Figure 9), and we therefore refer to these characteristic temperature values as "critical points".

KINETICS AND METASTABILITY

The observation that the model does not adopt its global minimal energy state at low temperatures in poor solvent (Figure 5B) indicates the metastable nature of initial conformations. It has previously been suggested that native helical secondary structure may resemble a metastable state which is kinetically "protected" from transformation into thermodynamically favored densely aggregated globular states.[45] This notion is supported by our Brownian dynamics trajectories recorded in the low-mid temperature range, which exhibit abrupt transitions between extended helical and condensed globular states (Figure 7).

At very low temperatures, the initial helical polymer conformation is kinetically trapped and no change is observed over the time of observation (Figure 7A). However, at temperatures greater than the critical point (200 K for an initial helix or straight chain), the barrier between helix and globule can be crossed within the simulation time frame, and a pronounced downward jump in radius of gyration and potential energy is seen, indicating adoption of a condensed globule (Figure 7B). At higher temperatures we find more frequent jumps with decreased magnitude, i.e. the reverse process also becomes apparent (see Figure 7C)—that is, a repeated switching between the helical and the globular state. Finally, at very high temperatures (1000 K and above in our simulations), barriers on the energy landscape become irrelevant, and the minimal polymer model adopts a random coil conformation (Figure 7D).

PHASE BEHAVIOR

As discussed in previous sections, the minimal model of a chiral polymer chain with intrinsic bend and torsion, investigated as a function of temperature and effective solvent conditions, is capable of adopting several distinct conformational states. We asked whether the transformations between those may represent true *thermodynamic phase transitions* commonly defined by nonanalytic behavior of free energy as a function of a thermodynamic variable—and if so, how they can be classified.[46] Notably, there currently is no general agreement whether a single-chain transformation, such as the one between helix and random coil, may be referred to as a thermodynamic phase transition or not. It is questionable whether a single polymer chain composed of a finite number of residues (N = 100 in our case) represents a *phase* in the sense of a thermodynamic limit of microstates with essentially uniform physical properties,[47] but an extrapolative approximation may be yielded by means of finite-size scaling analysis. According to

dx.doi.org/10.1021/ma500720t | *Macromolecules* 2014, 47, 6086−6094

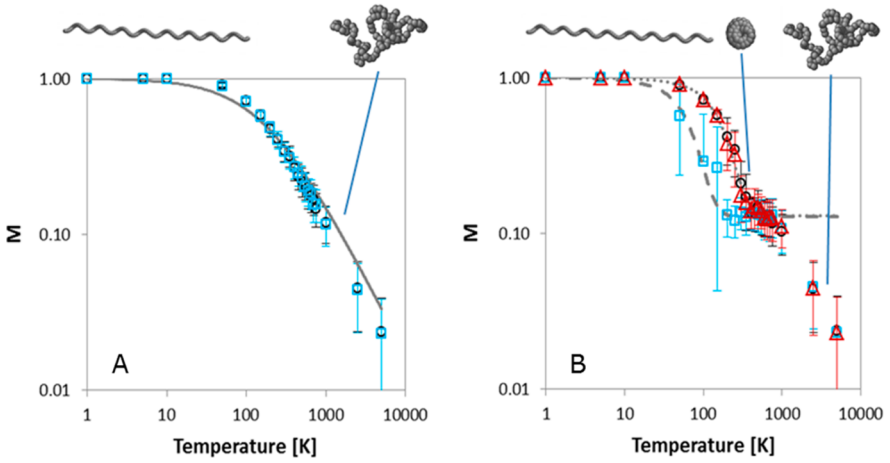

Figure 8. Equilibrium order parameter M as a function of temperature for initial helix (black circle), initial random coil (blue square), and initial straight chain (red triangle) in (A) near-Θ solvent ε_r, or (B) poor solvent ε_a. Fits by an empirical functions $M(T) = 1/[1 + (T/172)]$ (solid gray line), $M(T) = 0.13 + 1/\{1 + 2.8 \times \exp[(T - 200)/67.5]\}$ (dotted gray line), and $M(T) = 0.13 + 1/\{1 + 3.58 \times \exp[(T - 84.5)/26.4]\}$ (dashed gray line) each satisfy an R^2 value of at least 0.99.

the Peierls argument, the classical Zimm–Bragg[15] and Lifson–Roig[16] helix–coil models derived from the 1D-Ising model[14] cannot undergo a phase transition: thermal fluctuations at finite temperature in one-dimensional systems are too high and no long-range order is established.[48] In light of this view, the transformation between helix and random coil essentially resembles a crossover, a continuous change in macroscopic physical parameters described by a sigmoid curve. However, it has more recently been argued that the one-dimensional description of a linear chain based on a sequence of coupled spin-flips may be too simplistic to capture the physical reality of the process.[19] In fact, a polymer is subject to long-range interactions between residues, and changes from a disordered coil to an ordered folded state in three-dimensional space, principally allowing long-range order and the incidence of phase transition-like behavior. The simulation framework employed here represents a suitable abstraction of this reality. To investigate the nature of the helix–coil and helix–globule state transformations, we examined an appropriate order parameter representing the average helicity (phase chirality) as a local thermodynamic average of relevant structural features. This approach leaves conformational order independent from the number of residues, and allows extrapolation of results to the thermodynamic limit of an infinitely long chain. Inspired by the classical helix–coil models, the order parameter

$$M = \frac{h}{N - 2} \tag{9}$$

with number of nonterminal *helical* residues h and total number of chain residues N counts monomer properties characteristic of a well-ordered helix. Terminal residues may move freely, are not part of the helical segment and are therefore disregarded. According to this definition, $M = 1$ indicates a fully helical conformation, $M = 0$ one without any helical segments. Here, a residue is considered *helical* if both its bond- and torsional angles are within 10° of their respective target values (i.e., $|\theta - \theta_0| < 10°$ and $|\varphi - \varphi_0| < 10°$). This definition of a helical residue is stricter than in previous related work.[19,31] The resulting dependence of the order parameter $M(T)$ is shown in Figure 8, for an initial chain starting from the helix, straight-chain, and random coil conformations, under near-Θ and poor solvent conditions previously described. The subsequent fitting of these data is described in the figure caption, and reveals the two separate processes taking place at high temperatures, and around 200 K, respectively.

In Θ solvent, the order parameter M continuously decreases over temperature as the ordered helix transforms into a random coil (Figure 8A). As previously noted, the equilibrium behavior appears independent from initial chain conformation in this case. At high temperatures, the chain in the domain of a random coil is subject to an entropy maximization, which is characterized by simple power law dependence $M(T) \propto 1/T$. Overall, the near-Θ solvent behavior is well fit by the function $M(T) = 1/[1 + (T)/(172)]$, suggesting a single-process crossover between low and high temperature domains.

In poor solvent, $M(T)$ is shaped by two superimposed processes: the helix–coil transformation represented by a crossover as outlined above, and the helix–globule transition in the low-medium temperature range (Figure 8B). The latter process is well fit by a logistic function $M(T) = 0.13 + 1/\{1 + a \times \exp[(T - b)/c]\}$ characterized by steep exponential decline of the order parameter near the transition point and a plateau at $M = 0.13$, suggesting residual order within the condensed globule. As previously noted for thermodynamic properties (Figure 5), the helix–globule transition is observed at lower temperature if simulations start from a random coil compared to an initial helix or straight polymer chain. As expected, at high temperatures all these differences disappear and the system exhibits entropic power law dependence $M(T) \propto 1/T$ irrespective of the effective solvent environment or the initial conformation.

If we suspect a thermodynamic phase transformation is taking place,[49] the next step is to examine how the thermal fluctuations shape the average specific heat of the system. We calculate the heat capacity in the standard way, via the variance of the internal energy fluctuations,

$$C_N = \frac{\langle PE^2 \rangle - \langle PE \rangle^2}{N(k_B T)^2} \tag{10}$$

as a function of temperature. Plotting this in Figure 9, we find a very sharp peak in specific heat reminiscent of a discontinuity at approximately 50 K for an initial random coil, and a similar feature at 200 K for an initial helix or straight chain under poor

dx.doi.org/10.1021/ma500720t | *Macromolecules* 2014, 47, 6086–6094

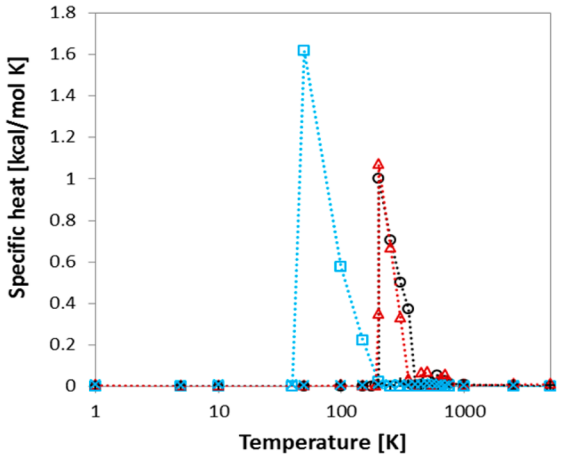

Figure 9. Specific heat as a function of temperature for initial helix in near-Θ solvent (black plus), initial helix in poor solvent (black circle), initial random coil in near-Θ solvent (blue cross), initial random coil in poor solvent (blue square, rescaled 1/10), and initial straight chain (red triangle). To investigate the sharpness of the $C(T)$ anomaly, the temperature step during the jump was 10 K.

solvent conditions. These anomalies correspond well to the crossover temperatures seen in the order parameter variation $M(T)$ in Figure 8B, illustrating once more that characteristic temperature of helix−globule transition is lower if simulations start from a random coil configuration, compared to an extended initial chain.

No thermodynamic anomaly was seen in near-Θ solvent, where only the helix−coil transformation is taking place. In contrast, a pronounced peak in $C(T)$ is seen in poor solvent conditions, with the essentially step-like jump at the low-T edge (herein referred to as "critical point"), which must be linked to the helix−globule transition. Peaks in heat capacity generally indicate pronounced fluctuations in the system energy as a function of temperature, irrespective of the nature of state transformation. Given the fact that we do not observe a transition until temperature allows sufficient flexibility in a natively helical chain, and the transformation from helix to coil is continuous (as seen in the near-Θ solvent data), we may in fact refer to the helix−globule transition as an instance of discontinuous coil−globule collapse.

CONCLUSION

We have examined a minimal model of an intrinsically helical polymer embracing transparently adjustable curvature and torsion as a measure of residue-inherent chirality, and investigated its phase behavior by means of Brownian dynamics simulation. In near-Θ solvent, the helical ground state is continuously dissolved toward a random coil through a smooth crossover between low and high temperature regime. This transformation is found to be reversible and not dependent on the initial conformation we start the simulations with. In contrast, in poor solvent characterized by a significant long-range attraction between chain residues, the above helix−coil transformation is superimposed by a sharp discontinuous helix−globule collapse in the low-mid temperature range. On the basis of the data for the average chain potential energy, its radius of gyration, and the specific heat, as functions of temperature, we suggest that this transformation resembles a thermodynamic phase transition driven by thermal fluctuations, which is supported by previous experimental data, numerical simulations, and the theory of semiflexible polymers.[32,34,50,51] Conformational intermediates captured during the helix−globule collapse indicate that it proceeds via nucleation initiated at the polymer termini, so that the chain subsequently collapses into the globule alongside its axis. This process is reminiscent of the Halperin−Goldbart mechanism,[39,43] whereby sufficiently flexible polymer chains collapse into terminal "raindrops" in the short-chain limit.

Interestingly, an initial random coil conformation is found to collapse into a globule at significantly lower temperatures than an initial helix or straight chain (all in poor solvent). This observation supports the notion that native helical secondary structure in natural biopolymers, especially polypeptides and proteins, represents a deep metastable state which protects the polymer from transition into thermodynamically favored aggregate conformations. We confirm the metastable nature of initial conformations in deteriorated solvent by means of Brownian dynamics trajectories, whereby spontaneous transitions between apparently coexisting extended and condensed conformations become apparent via pronounced jumps in compactness and potential energy as temperature is high enough for energy barriers to be crossed.

It is an interesting notion that the qualitative robustness in thermodynamic properties and phase behavior enabled by intrinsic helicity, regardless of specific chemistry, may be the basis of the prevalence of helical conformations in natural biopolymers. Future studies of chains embracing different lengths, stiffness, and implementations of intrinsic curvature and torsion would supplement our conclusions on the nature of transitions between helix, globule, and coil, and address the question how the phase behavior of a polymer may be modulated by its monomer's chirality properties.

AUTHOR INFORMATION

Corresponding Author

*(E.M.T.) E-mail: emt1000@cam.ac.uk.

Notes

The authors declare no competing financial interest.

ACKNOWLEDGMENTS

The authors wish to acknowledge A. Lappala and O. T. Strickson for providing an introduction to LAMMPS. This work was kindly supported by a Lloyd's Register Educational Trust Scholarship (to C.R.B.) and carried out within the Cavendish Centre for Scientific Computing (N. Nikiforakis).

REFERENCES

(1) Banavar, J.; Maritan, A. *Annu. Rev. Biophys. Biomol. Struct.* **2007**, *36*, 261−280.
(2) Anfinsen, C. B. *Science* **1973**, *181*, 223−230.
(3) Fodje, M. N.; Al-Karadaghi, S. *Protein Eng.* **2002**, *15*, 353−358.
(4) Seol, Y.; Skinner, G. M.; Visscher, K.; Buhot, A.; Halperin, A. *Phys. Rev. Lett.* **2007**, *98*, 158103−158107.
(5) Sugimoto, N.; Nakano, S.; Katoh, A.; et al. *Biochemistry* **1995**, *34*, 11211−11216.
(6) Varshavsky, A. *Cell* **2006**, *127*, 1295−1297.
(7) Watson, J. D. *Molecular Biology of the Gene*; Cold Spring Harbor Laboratory Press: New York, 2003.
(8) Berg, J. M.; Tymoczko, J. L.; Stryer, L. *Stryer Biochemie*; Elsevier: Munich, 2007.
(9) Ho, R. M.; Li, M. C.; Lin, S. C.; et al. *J. Am. Chem. Soc.* **2012**, *134*, 10974−10986.
(10) Pauling, L.; Corey, R. B.; Branson, H. R. *Proc. Natl. Acad. Sci. U.S.A.* **1951**, *27*, 205−211.

(11) Poland, D.; Scheraga, H. A. *Theory of Helix Coil Transitions in Biopolymers*; Academic Press: New York, 1970.
(12) Doig, A. J. *Biophys. Chem.* **2002**, *101*, 281−293.
(13) Doig, A. J. *Protein Folding, Misfolding and Aggregation: Classical Themes and Novel Approaches*; Royal Society of Chemistry: London, 2008.
(14) Ising, E. *Z. Phys.* **1925**, *31*, 253−258.
(15) Zimm, B. H.; Bragg, J. K. *J. Chem. Phys.* **1959**, *31*, 526−536.
(16) Lifson, S.; Roig, A. *J. Chem. Phys.* **1960**, *34*, 1963−1974.
(17) Doig, A. J.; Baldwin, R. L. *Protein Sci.* **1995**, *4*, 1325−1336.
(18) Mermin, N. D.; Wagner, H. *Phys. Rev. Lett.* **1966**, *17*, 1133−1136.
(19) Hansmann, U. H. E.; Okamoto, Y. *J. Chem. Phys.* **1999**, *110*, 1267−1277.
(20) Peyrard, M.; Bishop, A. R. *Phys. Rev. Lett.* **1989**, *62*, 2755−2758.
(21) Pasteur, L. *Ann. Chim. Phys.* **1848**, *24*, 442.
(22) Wu, M.; Walker, S. I.; Higgs, P. G. *Astrobiology* **2012**, *12*, 818−829.
(23) Yashima, E.; Maeda, K.; Okamoto, Y. *Nature* **1999**, *399*, 449−451.
(24) Zhang, J.; Bu, X. *Chem. Commun.* **2009**, *2*, 206−208.
(25) Ripoll, D. R.; Scheraga, H. A. *Biopolymers* **1988**, *27*, 1283−1303.
(26) Wilson, S. R.; Cui, W. *Biopolymers* **1990**, *29*, 225−235.
(27) Kawai, H.; Okamoto, Y.; Fukugta, M.; Nakazawa, T.; Kikuchi, T. *Chem. Lett.* **1991**, *2*, 213−216.
(28) Okamoto, Y. *Proteins Struct. Funct. Genet.* **1994**, *19*, 14−23.
(29) Sung, S. S. *Biophys. J.* **1995**, *68*, 826−834.
(30) Kemp, J. P.; Chen, Z. Y. *Phys. Rev. Lett.* **1998**, *81*, 3880−3883.
(31) Kemp, J. P.; Hansmann, U. H. E.; Chen, Z. Y. *Eur. Phys. J. B* **2000**, *15*, 371−374.
(32) Kemp, J. P.; Chen, J. Z. Y. *Biomacromolecules* **2001**, *2*, 389−401.
(33) Varshney, V.; Dirama, T. E.; Sen, T. Z.; Carri, G. A. *Macromolecules* **2004**, *37*, 8794−8804.
(34) Varshney, V.; Carri, G. A. *J. Chem. Phys.* **2007**, *126*, 044906.
(35) Yamakawa, H.; *Helical Wormlike Chains in Polymer Solutions*; Springer: Berlin, 1999.
(36) Craig, A.; Terentjev, E. M. *Macromolecules* **2006**, *39*, 4557−4565.
(37) Kremer, K.; Grest, G. S. *J. Chem. Phys.* **1990**, *92*, 5057.
(38) MacKerell, A. D., Jr.; Bashford, D.; Bellott, M.; et al. *J. Phys. Chem. B* **1998**, *102*, 3586−3616.
(39) Lappala, A.; Terentjev, E. M. *Macromolecules* **2013**, *46*, 1239−1247.
(40) Plimpton, S. *J. Comput. Phys.* **1995**, *117*, 1−19.
(41) Schneider, T.; Stoll, E. *Phys. Rev. B* **1978**, *17*, 1302−1322.
(42) Beisbart, C.; Hartmann, S. *Probabilities in Physics*; Oxford University Press: Oxford, U.K., 2010.
(43) Halperin, A.; Goldbart, P. M. *Phys. Rev. E* **2000**, *1*, 565−573.
(44) Kikuchi, N.; Ryder, J.; Pooley, C.; Yeomans, J. *Phys. Rev. E* **2005**, *71*, 061804.
(45) Ricchiuto, P.; Brukho, A. V.; Auer, S. *J. Phys. Chem. B* **2012**, *116*, 5384−5390.
(46) Blundell, J. S.; Blundell, K. M. *Concepts in Thermal Physics*; Oxford University Press: Oxford, U.K., 2008.
(47) Modell, M.; Reid, R. C. *Thermodynamics and its Applications*: Prentice-Hall: Englewood Cliffs, NJ, 1974.
(48) Peierls, R. *Math. Proc. Camb. Philos. Soc.* **1936**, *3*, 477−481.
(49) Ehrenfest, P. *Proc. R. Acad. Amst.* **1933**, *36*, 153−157.
(50) Haran, G. *Curr. Opin. Struct. Biol.* **2012**, *22*, 14−20.
(51) Grosberg, A. Y.; Kokhlov, A. R.*Statistical Physics of Macromolecules*Am. Inst. of Phys.: Melville, NY, 1994.